

The Cassini 2000 Solar Conjunction: Ka-band and X-band Signal Propagation Through the Solar Corona

David Morabito,

Shervin Shambayati, Susan Finley, and David Fort

Jet Propulsion Laboratory

California Institute of Technology

American Geophysical Union

Spring 2001 Meeting

Paper SH32B-02

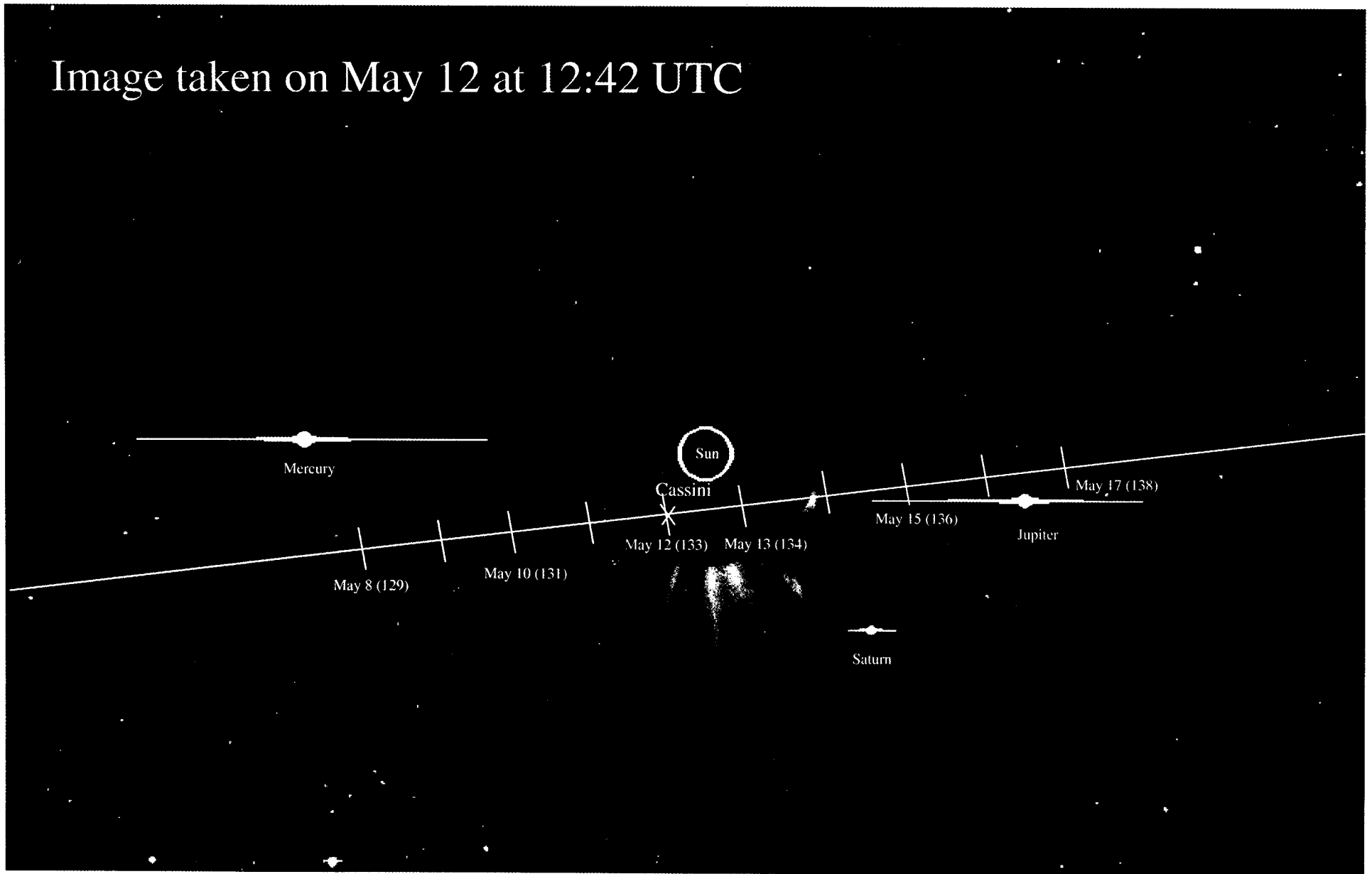
May 30, 2001

Background

- **This experiment was part of a telecommunications demonstration to evaluate the advantage of Ka-band (32 GHz) over X-band (8.4 GHz)**
- **An analysis of simultaneous Ka-band and X-band Mars Global Surveyor (MGS) data acquired from 1996 to 1998 demonstrated a 6 to 8 dB link advantage using a 34-m beam waveguide (BWG) ground antenna**
- **As part of the dual-frequency X/Ka link experiment, observations were made of several spacecraft during their solar conjunctions to study charged particle effects.**
 - For spacecraft passages behind the Sun's corona, the signals will encounter significant degradation due to charged particle density variations
 - Ka-band will have significantly less amplitude and phase scintillation than X-band
- **The Cassini May 2000 solar conjunction was the second in which simultaneous X-band and Ka-band data were acquired**
 - This superior conjunction occurred near the peak of the current solar cycle
 - Observable quantities include
 - Amplitude Scintillation
 - Phase Scintillation
 - Spectral broadening

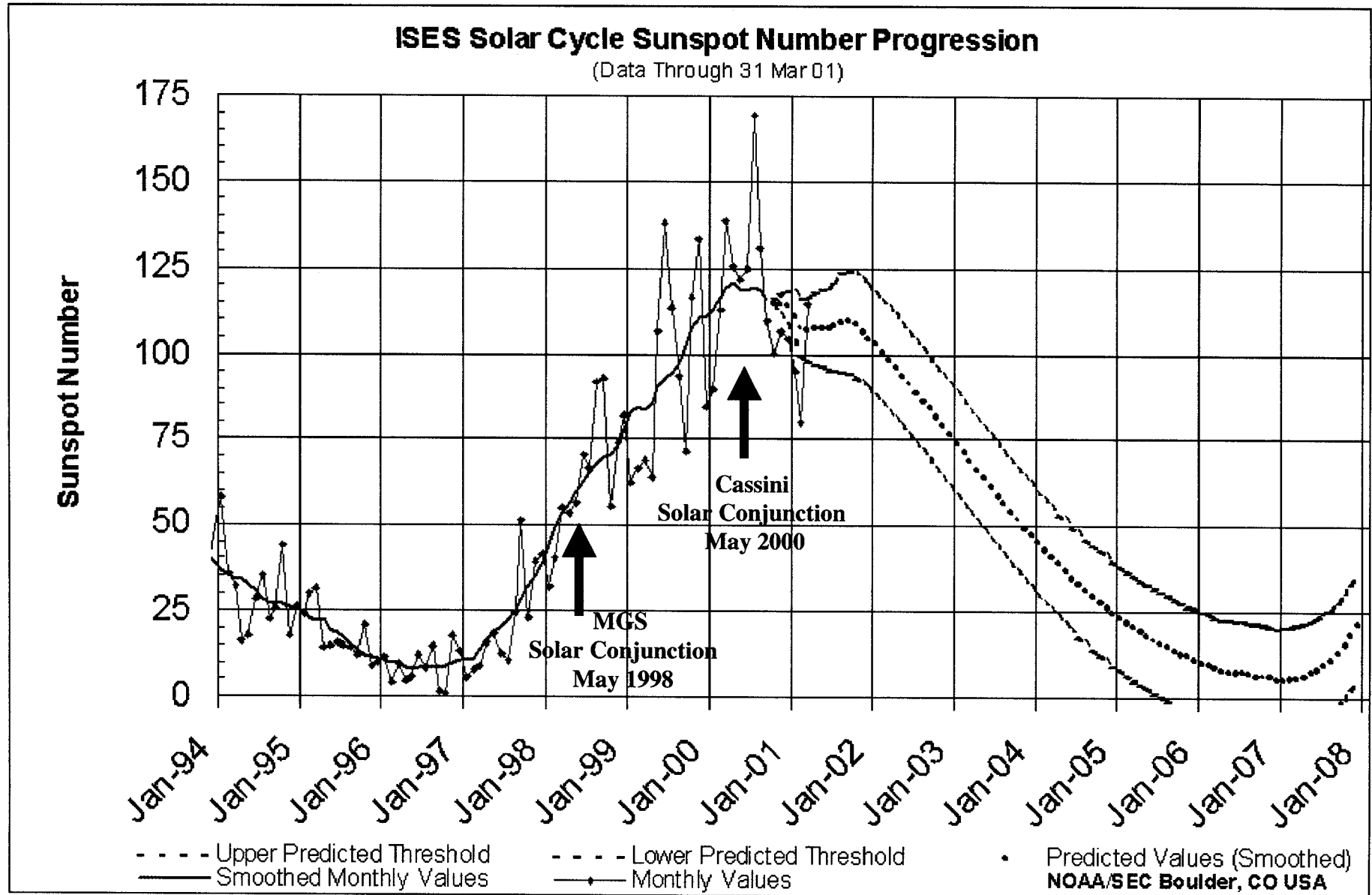
SOHO LASCO Image with Cassini Trajectory

Image taken on May 12 at 12:42 UTC



The SOHO/LASCO data used here are produced by a consortium of the Naval Research Laboratory (USA), Max-Planck-Institut fuer Aeronomie (Germany)), Laboratoire d'Astronomie (France), and the University of Birmingham (UK). SOHO is a project of international cooperation between ESA and NASA.

Sunspot Number versus time



Plot created by U. S. Department of Commerce, National Oceanic and Atmospheric Administration (NOAA), Space Environmental Center (web site at <http://sec.noaa.gov>).

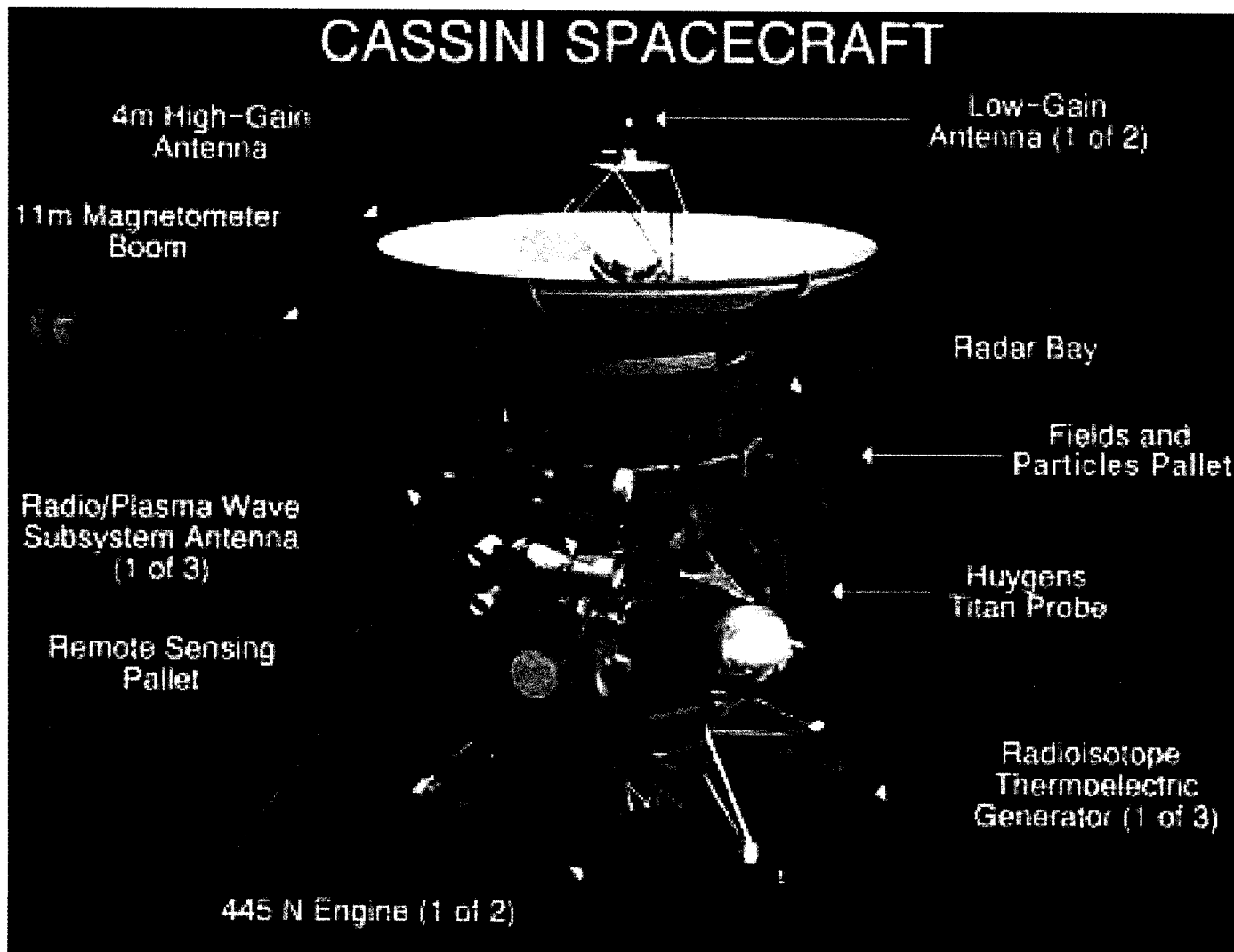
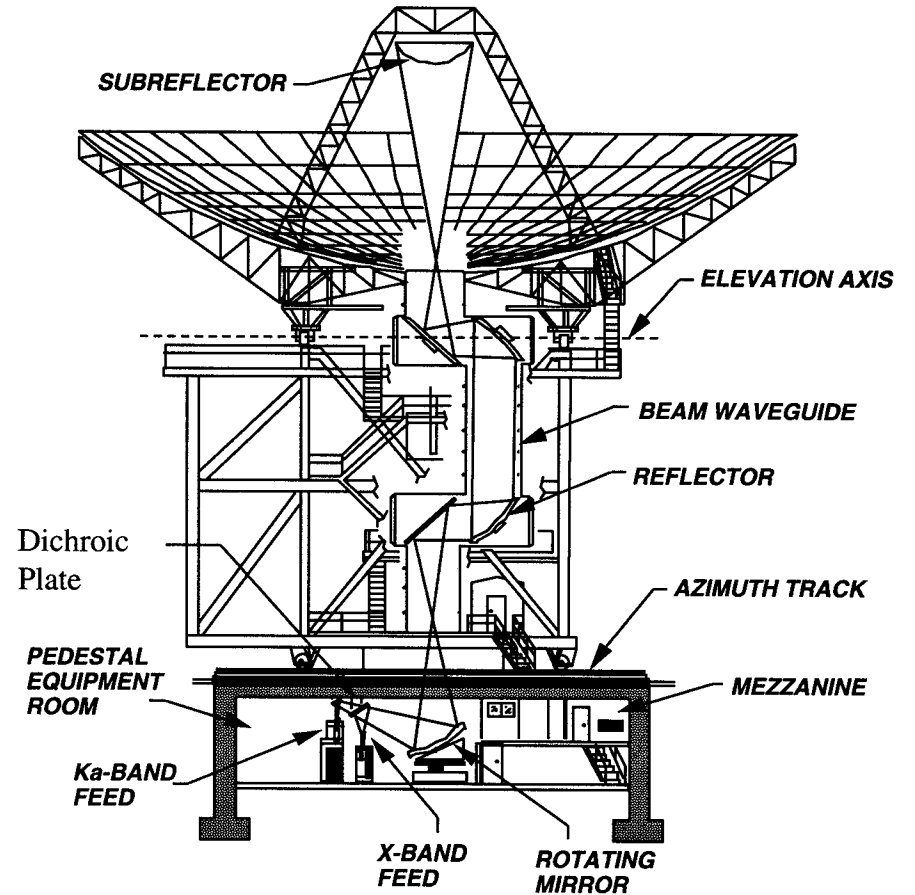
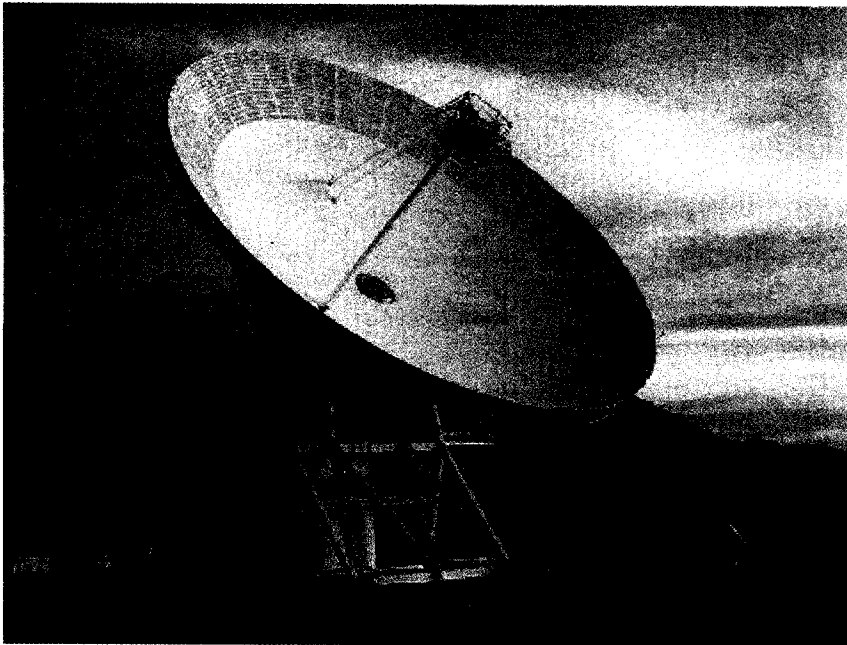


Photo Credit:

http://www.jpl.nasa.gov/cassini/english/pic/cassini_slide_set.html

DSS-13: The Goldstone R&D Beam Waveguide (BWG) Antenna



Signal Strength versus Solar Elongation Angle

May 13, 2000
2000-134
SEP=0.6°

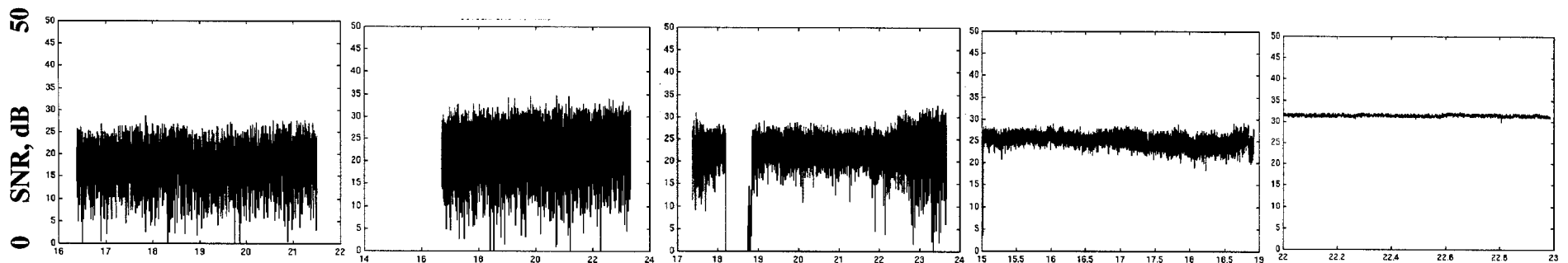
May 14, 2000
2000-135
SEP=1.1°

May 15, 2000
2000-136
SEP=1.8°

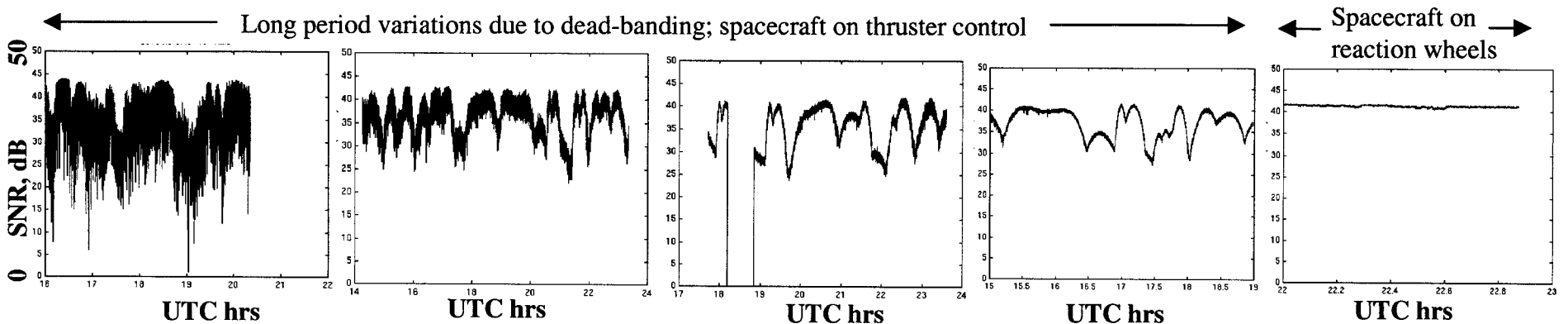
May 17, 2000
2000-138
SEP=3.1°

June 16, 2000
2000-168
SEP=23.8°

X-band SNR

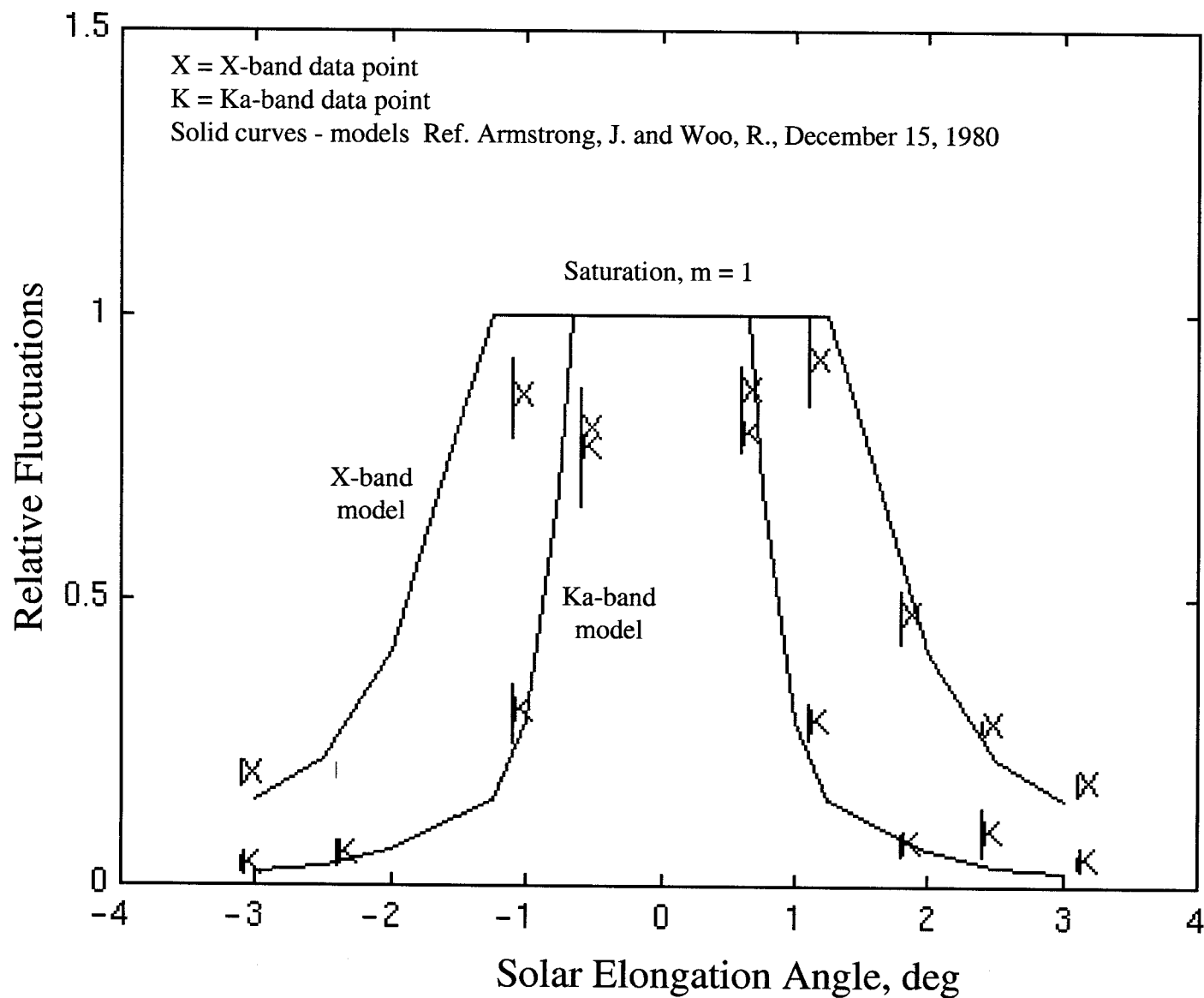


Ka-band SNR



Cassini 2000 Solar Conjunction

Relative Signal Power Fluctuations (rms/mean)



Frequency Residuals versus Solar Elongation Angle

May 13, 2000
2000-134
SEP=0.6°

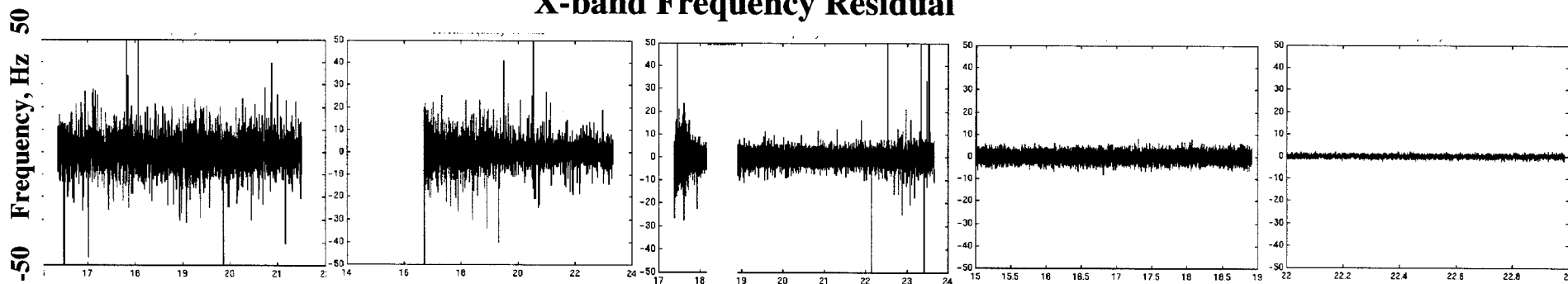
May 14, 2000
2000-135
SEP=1.1°

May 15, 2000
2000-136
SEP=1.8°

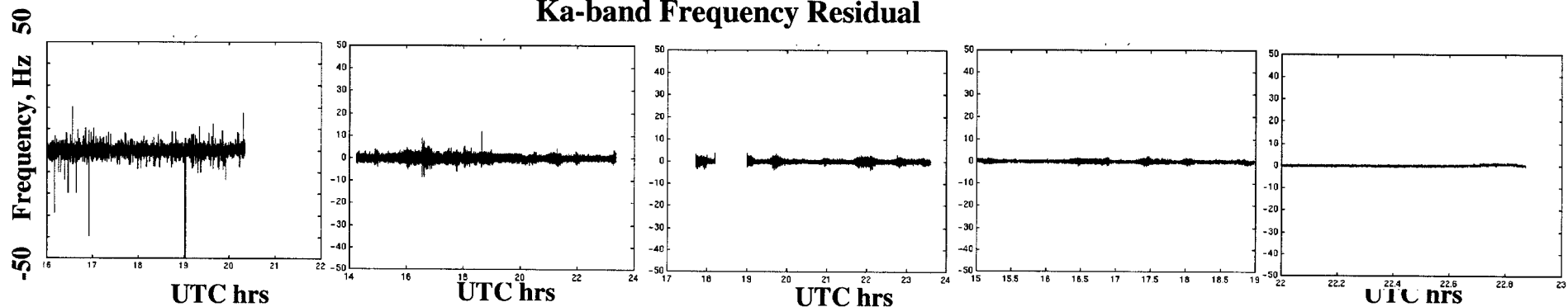
May 17, 2000
2000-138
SEP=3.1°

June 16, 2000
2000-168
SEP=23.8°

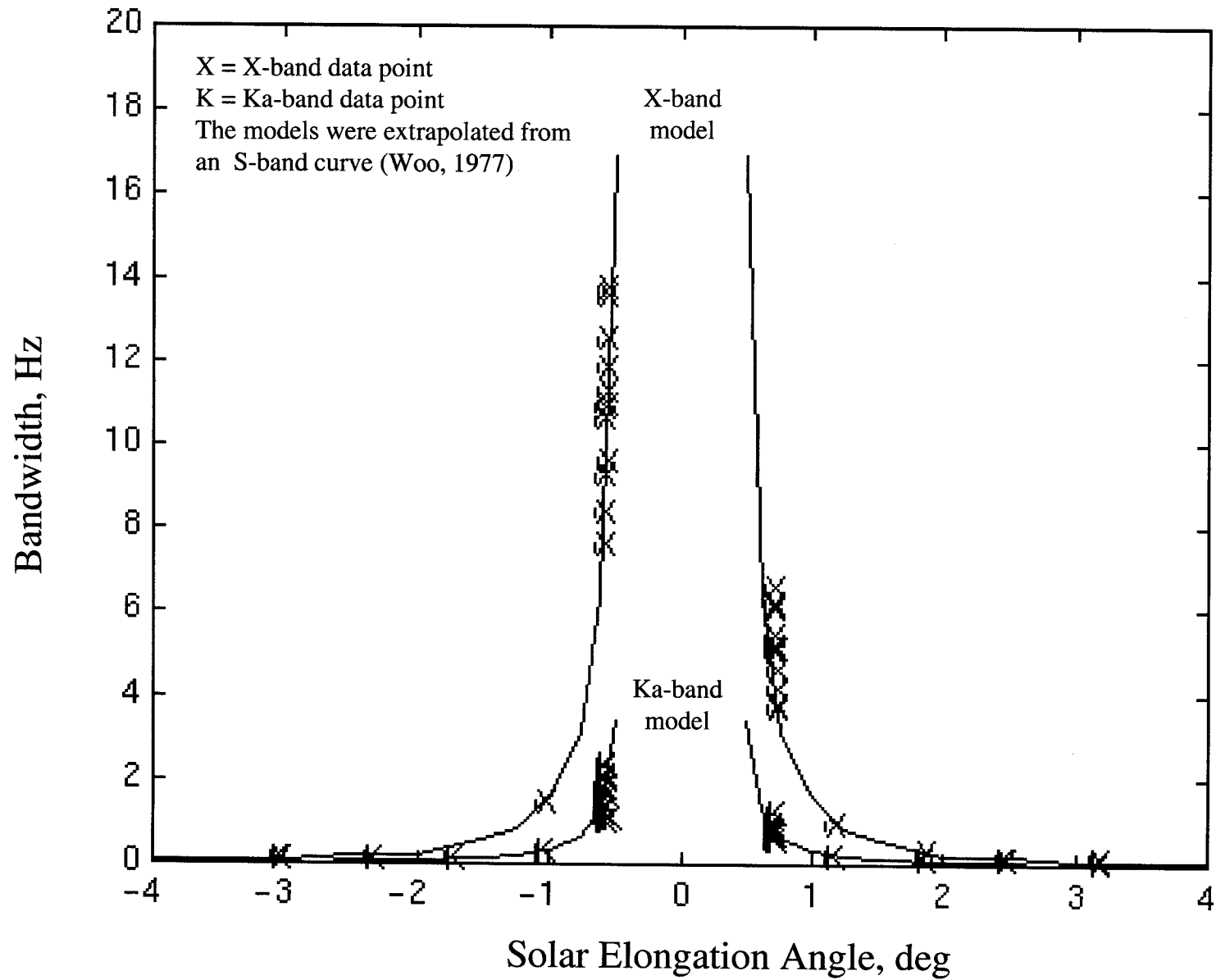
X-band Frequency Residual



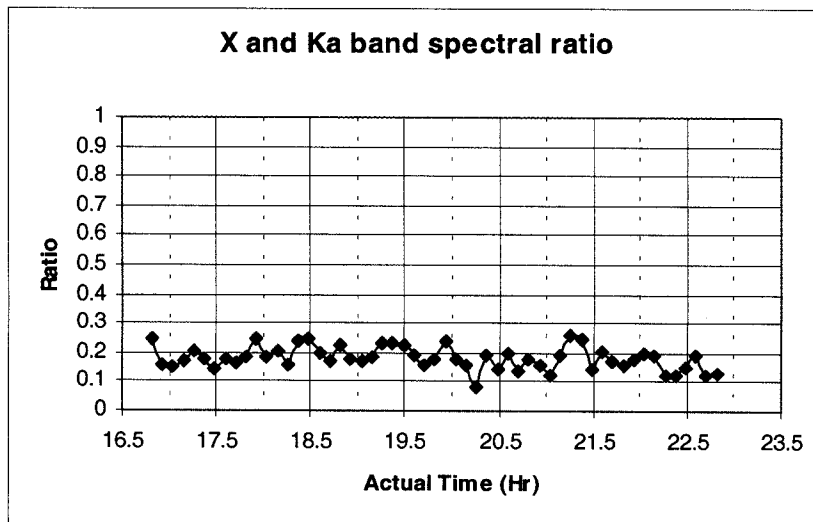
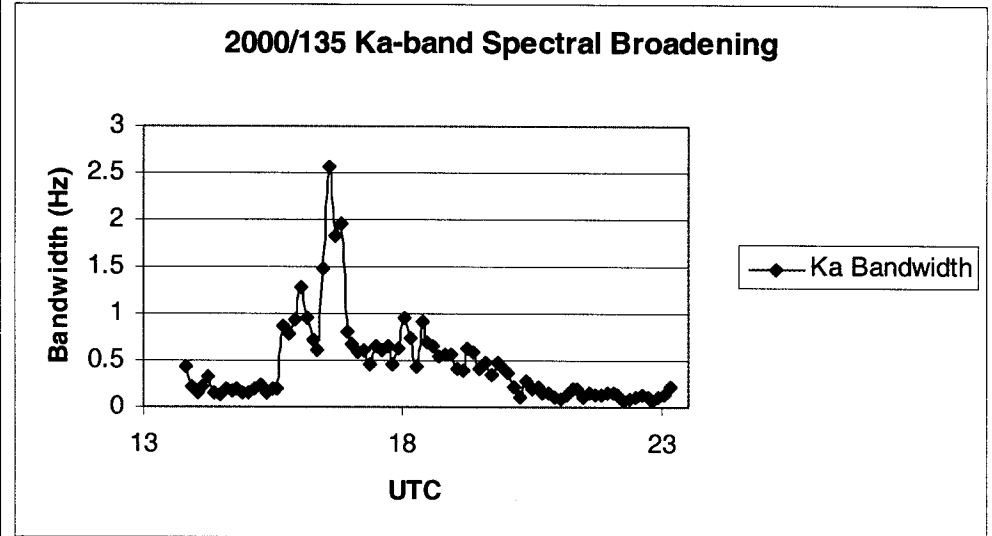
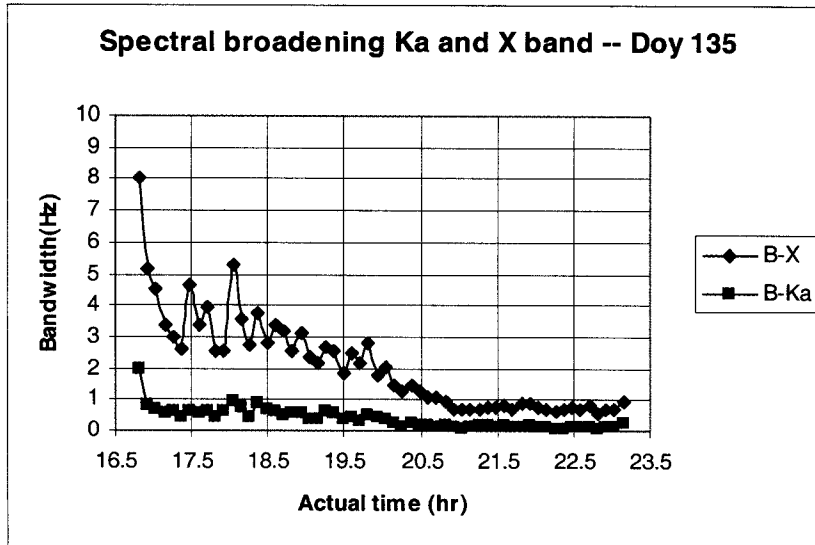
Ka-band Frequency Residual



Cassini 2000 Solar Conjunction Spectral Broadening



Spectral Broadening for pass 2000/135 (May 14) Egress 1.1° SEP Pass



Cassini 2000/136 (May 15)

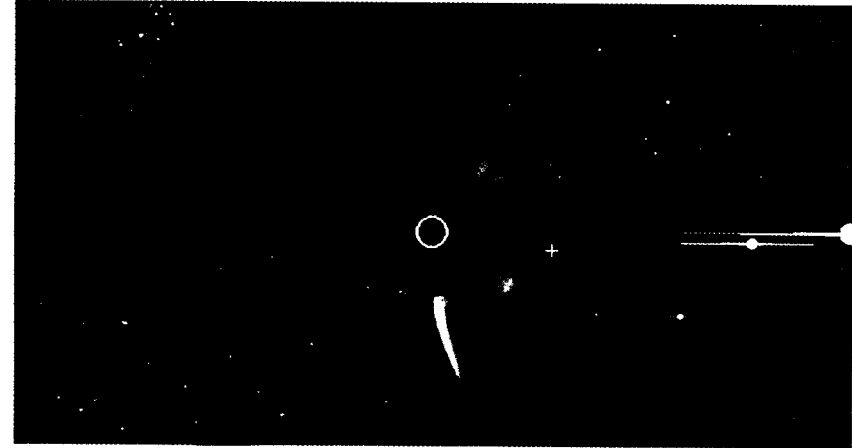
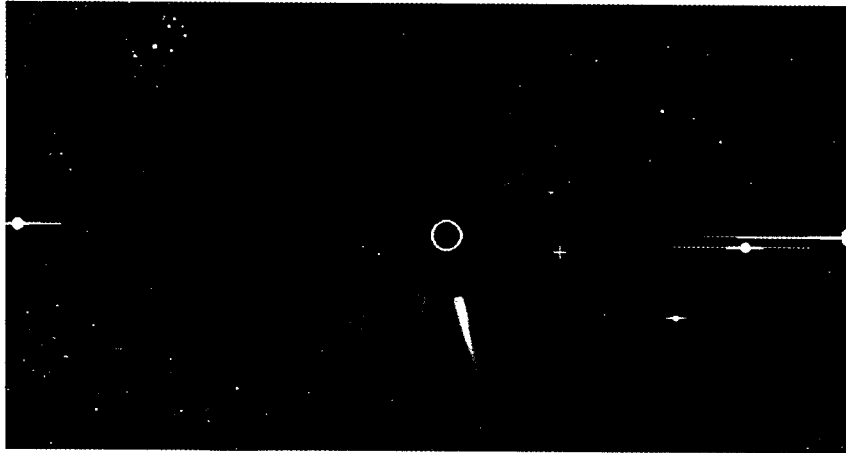
Before Event

SEP = 1.8°

Event Captured

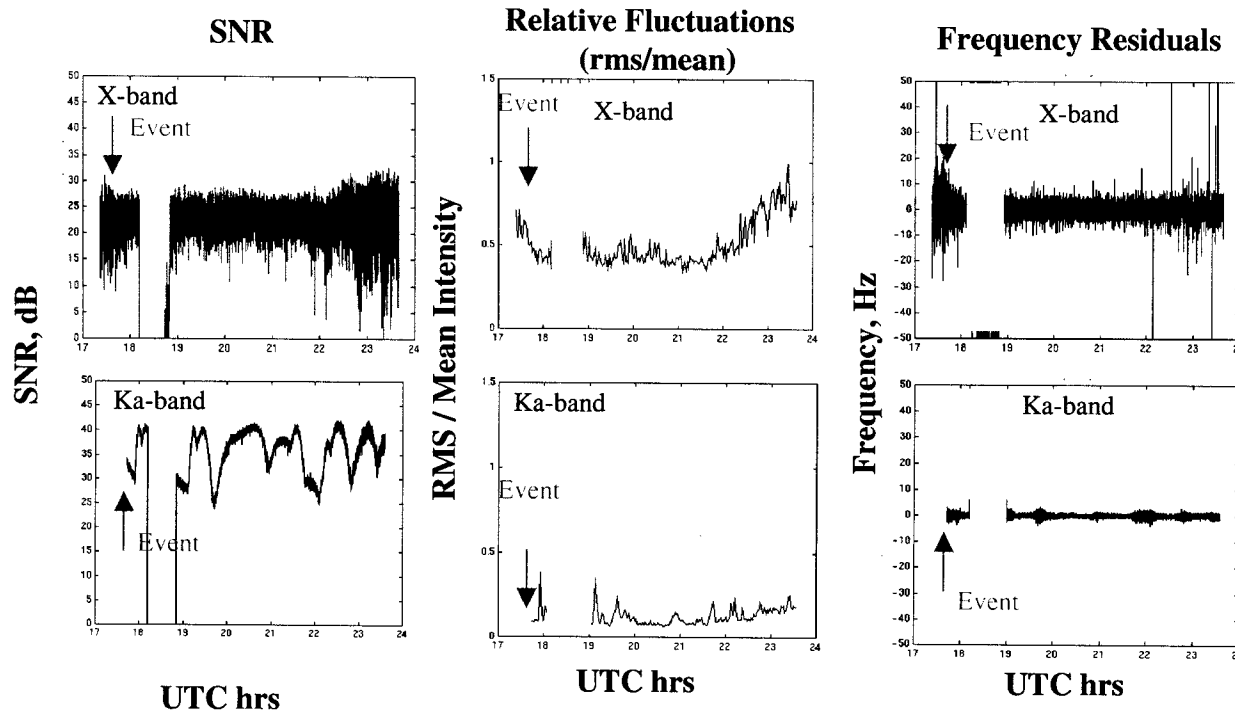
LASCO C3 Image 12:42 UTC

LASCO C3 Image 17:42 UTC



http://sohowww.nascom.nasa.gov/data/summary/gif/20000515/slas_c3wlc_fd_20000515_1242.gif

http://sohowww.nascom.nasa.gov/data/summary/gif/20000515/slas_c3wlc_fd_20000515_1742.gif



Solar event observed in Cassini 2000/136 data ~ 17:30 UTC was captured in a LASCO image taken at 17:42 UTC (the approximate location of the Cassini spacecraft is indicated by the "+")

This event is characterized by both intensity and frequency fluctuations.

The Ka-band SNR long period variations are due to spacecraft dead-banding

Another solar event starting at near 22:00 UTC is also apparent.

Conclusions

- The Cassini Solar Conjunction in May 2000 was the second in which simultaneous Ka-band and X-band carrier data were acquired
- The measured effects of solar charged particles on the carrier signals versus solar elongation angle were consistent with predictions based on models derived from theory and previous solar conjunction data
- A significant number of transient events were observed
 - Transient and quiescent periods of spectral broadening bandwidth measurements were compared for small solar elongation angles
 - Transient activity periods occurred 36% of the time

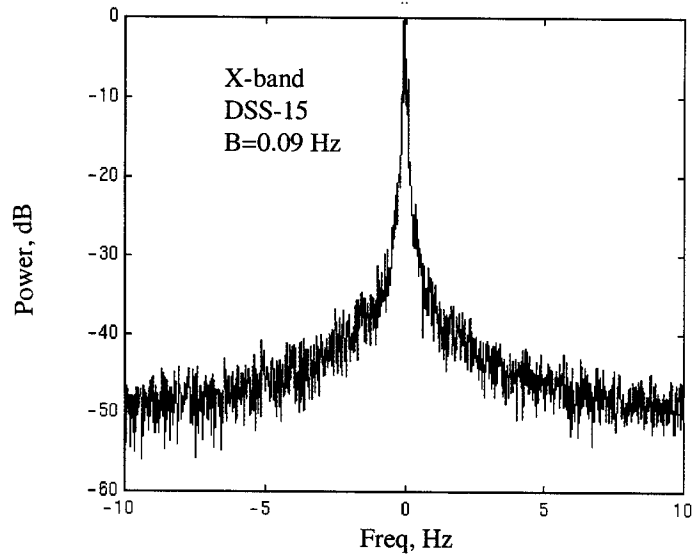
Backup Slides to Follow

Solar Effects on Signal Propagation

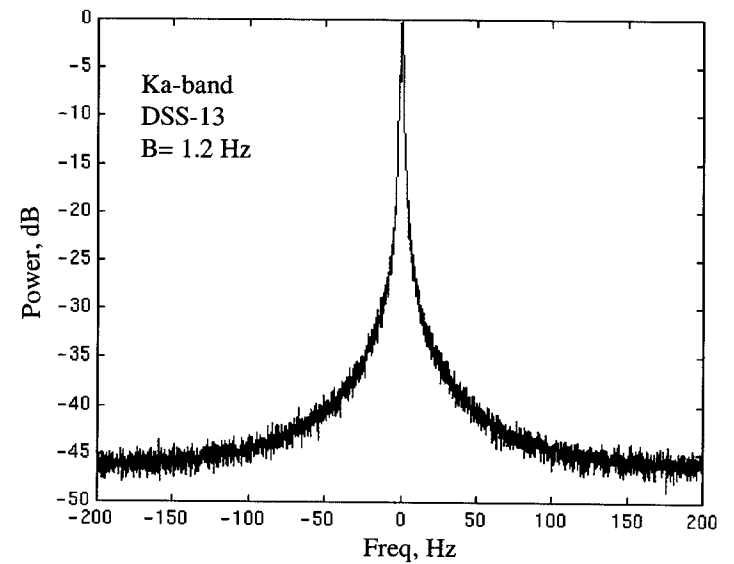
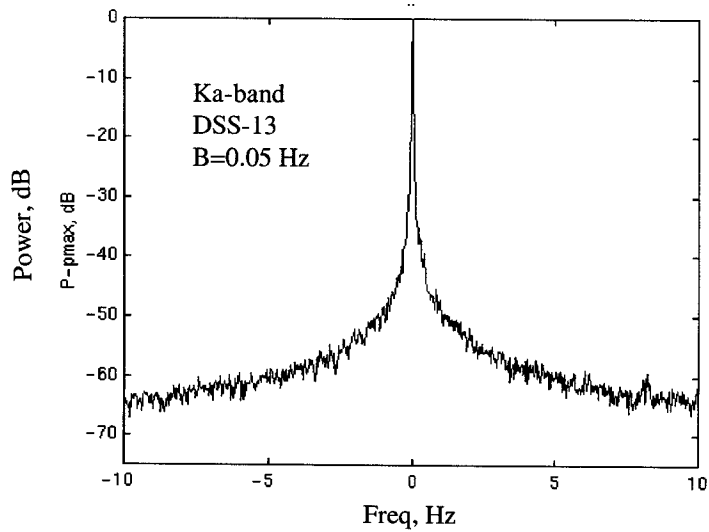
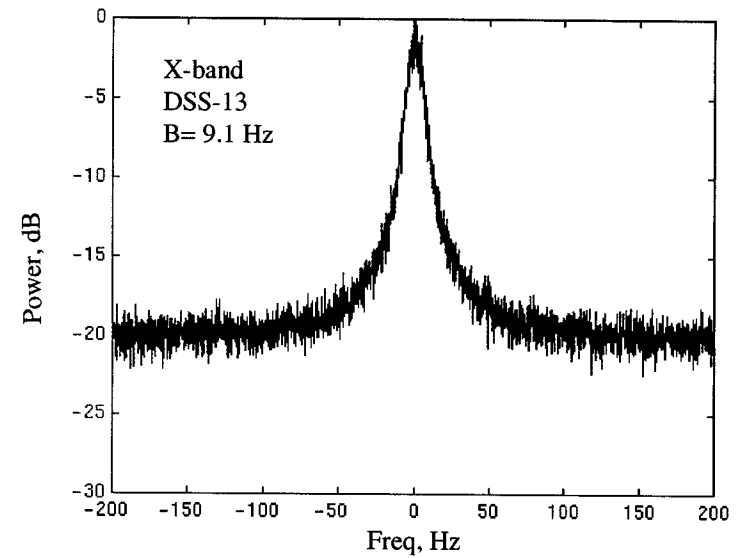
- Reduction of received signal power due to
 - angular broadening (if receive antenna beamwidth is too narrow)
 - spectral broadening (if receiver loop bandwidth is too narrow)
- Increased noise (contribution to Top increases with decreased SEP)
- Scintillation
 - fades on received signal power due to variations of charged particles within signal path
 - $m \sim k^{7/12} c_{no}$ Ref. Woo, R. 1977
 - for the same SEP angle, Ka-band fluctuations are less than X-band fluctuations ($m_{Ka} / m_x = 0.15$ in weak scintillation realm)
 - measurements compared with model from J. Armstrong and R. Woo 1980
- Spectral Broadening
 - spread of received signal power with frequency
 - dependent on both electron density fluctuations and solar wind velocity
 - $B \sim (c_{no} k)^{6/5} v$ Ref. Woo, R. 1977
 - $B_{Ka} = B_x / 3.8^{6/5} = 0.2 B_x$
 - Useful for scientific purposes when broadening exceeds linewidth of oscillator

Power Spectra of Cassini Carrier Signals

Power Spectra
Pass 2000/129 SEP = 3.1°



Power Spectra
Pass 2000/133 SEP = 0.6°



Transient Activity

- The spectral broadening bandwidth, B, due to solar effects is a good indicator of transient activity for small SEP angles as it does not saturate like the amplitude scintillation index, m
- Upon inspection of the spectral broadening bandwidth data, active periods were readily identified in which B increased above the quiescent background, peaked, and then settled back near the quiescent level
- Such active periods ranged from 19% to 50% of a pass for SEP angles between 0.6° to 1.8°

Day	SEP (deg)	#hours quiet	#hours active	% Active/Total
132	1.1	1.89	1.89	50
133	0.6	4.56	2.22	33
134	0.6	9.33	2.22	19
135	1.1	4.89	4.33	47
136	1.8	2.67	2.50	48
Total		23.3	13.2	36